

Section V

Accretion and Feeding

Chair: Tim Heckman

Accretion and Outflow in Active Galaxies

Andrew King¹

¹Theoretical Astrophysics Group, University of Leicester, Leicester LE1 7RH, UK
Email: ark@astro.le.ac.uk

Abstract. I review accretion and outflow in active galactic nuclei. Accretion appears to occur in a series of very small-scale, chaotic events, whose gas flows have no correlation with the large-scale structure of the galaxy or with each other. The accreting gas has extremely low specific angular momentum and probably represents only a small fraction of the gas involved in a galaxy merger, which may be the underlying driver.

Eddington accretion episodes in AGN must be common in order for the supermassive black holes to grow. I show that they produce winds with velocities $v \sim 0.1c$ and ionization parameters implying the presence of resonance lines of helium-like and hydrogen-like iron. The wind creates a strong cooling shock as it interacts with the interstellar medium of the host galaxy, and this cooling region may be observable in an inverse Compton continuum and lower-excitation emission lines associated with lower velocities. The shell of matter swept up by the shocked wind stalls unless the black hole mass has reached the value M_σ implied by the M - σ relation. Once this mass is reached, further black hole growth is prevented. If the shocked gas did not cool as asserted above, the resulting (“energy-driven”) outflow would imply a far smaller SMBH mass than actually observed. Minor accretion events with small gas fractions can produce galaxy-wide outflows, including fossil outflows in galaxies where there is little current AGN activity.

Keywords. accretion: accretion disks, galaxies: formation, galaxies: active, black hole physics

1. Accretion: Large-Scale

Accretion on to a black hole is the most efficient way of extracting energy from normal matter, and so must power the most luminous phenomena in the universe. To drive quasars and other bright AGN without exceeding the Eddington limit requires supermassive black hole (SMBH) accretors, ranging up to several $10^9 M_\odot$, and accretion rates of up to $10 M_\odot \text{ yr}^{-1}$. These statements probably encapsulate all that is securely known about accretion in AGN.

The M - σ relation (see below) strongly suggests a connection between SMBH and galaxy growth. This in turn points to galaxy mergers as the common motor of both phenomena. Cosmological simulations (e.g., Di Matteo *et al.* 2005) aim to show the plausibility of this idea, by demonstrating how a series of mergers can produce SMBH and galaxies satisfying the M - σ relation at low redshift. To make the calculations tractable requires a sub-resolution recipe for accretion, and this is usually taken as the Bondi rate

$$\dot{M}_B = 4\pi R_B^2 \rho c_s, \quad (1.1)$$

where

$$R_B = \frac{2GM}{c_s^2} \quad (1.2)$$

is the Bondi radius, with c_s the local sound speed, ρ the gas density and M the SMBH mass.

However there are several problems with this recipe. First, it is self-consistent only if M is a good approximation to the total gravitating mass inside R_B . This requires

$$R_B < \frac{GM}{2f_g\sigma^2} \sim 10 - 20 \text{ pc}, \quad (1.3)$$

where $f_g \approx 0.16$ is the gas fraction relative to dark matter, and σ is the velocity dispersion in the galaxy bulge. This is far smaller than the spatial resolution available in typical cosmological simulations. If the resolution scale is $R > R_B$, the recipe gives $\dot{M} \sim (R/R_B)^2 \dot{M}_B \gg \dot{M}_B$. This often leads to estimated accretion rates far above the Eddington rate \dot{M}_{Edd} , which have to be corrected by assuming that the rate never goes above this value. Although this may be roughly correct for bright quasars (see below), it is obvious that this arbitrary procedure must give an entirely misleading impression of the duty cycle of accretion.

In fact, it is unlikely that any AGN accretes at very super-Eddington rates. The maximum possible accretion rate is the dynamical value

$$\dot{M}_{\text{dyn}} \approx \frac{f_g \sigma^3}{2G}, \quad (1.4)$$

which describes the case where gas is initially in rough virial equilibrium in the bulge of a galaxy with velocity dispersion σ and baryonic mass fraction f_g . Parameterizing, we find

$$\dot{M}_{\text{dyn}} \approx 1.4 \times 10^2 \sigma_{200}^3 M_\odot \text{ yr}^{-1} \quad (1.5)$$

where $\sigma_{200} = \sigma/(200 \text{ km s}^{-1})$, and we have taken $f_g = 0.16$. For a black hole mass close to the observed M - σ relation, this implies an Eddington ratio

$$\dot{m} < \frac{\dot{M}_{\text{dyn}}}{\dot{M}_{\text{Edd}}} \approx \frac{33}{\sigma_{200}} \approx \frac{39}{M_8^{1/4}}, \quad (1.6)$$

where $M_8 = M/10^8 M_\odot$. Since $0.1 < M_8 < 10$ for the black holes in AGN, and \dot{M}_{dyn} is an upper limit to \dot{M} , modest values $\dot{m} \sim 1$ of the Eddington ratio are likely. Indeed, in the case where the SMBH does not dominate the mass inside the estimated Bondi radius, a realistic estimate of the Bondi rate is actually close to the dynamical value, since

$$\dot{M}_B = 4\pi R_B^2 \rho c_s = 3 \frac{M_g c_s}{R_B}, \quad (1.7)$$

where $M_g = 4\pi R_B^3 \rho/3$. Now using equation (1.2) with M_g in place of M , we see that

$$\dot{M}_B = \frac{3 c_s^3}{2 G}, \quad (1.8)$$

and in a realistic situation we would expect $c_s \sim \sigma$.

Even if one were able to resolve the Bondi radius and estimate the rate \dot{M}_B cleanly, it is still unlikely that this gives an estimate of the true accretion rate at the black hole and thus the AGN luminosity. The reason is that in any conceivable physical situation the gas must have sufficient angular momentum to orbit the black hole, and so must form an accretion disk. Thus the term ‘‘Bondi accretion’’ is better rendered as ‘‘Bondi capture.’’ Gas inside the Bondi radius cannot easily escape the black hole’s vicinity, but is not required to accrete on to it at the Bondi rate.

2. Accretion: Disks

The fact that accretion must ultimately proceed via a disk now leads to another set of difficulties. If, as is likely in many cases, the disk cools efficiently, it will become thin and Keplerian. In this case, we can compute its viscous timescale

$$\tau = \frac{R^2}{\nu} = \frac{2 \times 10^{10}}{\alpha_{0.1}} \left(\frac{R}{10^3 H} \right)^2 \frac{R_{\text{pc}}^{3/2}}{M_8^{1/2}} \text{ yr} \tag{2.1}$$

at disk radius $R = R_{\text{pc}}$ pc, where $\alpha_{0.1}$ is the viscosity parameter α in units of its likely value 0.1 (King *et al.* 2007), $H \approx 10^{-3} R$ is the disk scale height, and $M_8 = M/10^8 M_\odot$. So unless the disk is very small, its viscous time is too long for significant accretion on to the SMBH. If the disk is large, on the other hand, it is likely to become self-gravitating and fragment into stars, since its mass M_{disk} exceeds the self-gravity limit $\sim (H/R)M$, i.e.,

$$\frac{M_{\text{disk}}}{M} \frac{R}{H} = \frac{0.2}{\alpha_{0.1}} \left(\frac{R}{10^3 H} \right)^3 \left(\frac{R_{\text{pc}}}{M_8} \right)^{3/2} \frac{L}{L_{\text{Edd}}}. \tag{2.2}$$

Equation (2.1) shows that gas orbiting at only a few parsecs takes more than a Hubble time to accrete. So the gas which forms the disk and ultimately accretes must have arrived very close to the SMBH, with very little angular momentum. One would not expect such an accurate aim for most of the gas involved in a galaxy merger, so most of this gas evidently cannot accrete on to the SMBH. This is reasonable, given that we know (Håring & Rix 2004) that the mass of the black hole is only about 10^{-3} of the galaxy bulge’s baryonic mass. The merger process is evidently extremely inefficient in feeding the black hole, with most growing the bulge or other parts of the host galaxy.

Since the accretion disk is so small compared with the galaxy, and involves so little of the gas involved in a merger, this also suggests that its net angular momentum is likely to be uncorrelated with the large-scale structure of the host. Confirmation of this comes from the observed directions of AGN jets. As the jets are relativistic, they must be launched from the very near vicinity of the black hole, normal to the plane of the disk there. Their directions are observed to be uncorrelated with the galaxy structure (Kinney *et al.* 2000), just as the argument above suggests. Moreover, successive feeding events seem to produce jets whose directions deviate significantly from the previous ones.

We can now see an emerging picture of AGN accretion as a series of very small-scale, chaotic events, whose gas flows have no correlation with the large-scale structure of the galaxy or with each other. The feeding events must have extremely low specific angular momentum compared with that typical of the gas in a galaxy merger (King & Pringle 2006, 2007).

This picture does seem to work well in explaining some key features, in particular the evolution of mass and spin in SMBH, and the jet directions discussed above (King & Pringle 2006, 2007; King *et al.* 2008; Fanidakis *et al.* 2009). The key here is that the black hole spin specifies the efficiency η of luminous energy release by accretion, and thus the accretion luminosity

$$L_{\text{acc}} = \eta M c^2. \tag{2.3}$$

The higher the spin, the higher η , and thus the *lower* the rate at which the black hole mass can grow, because the accretion luminosity cannot greatly exceed the Eddington limit. Hence rapid black hole growth to high masses, as observed in some high-redshift quasars (Barth *et al.* 2003; Willott *et al.* 2003), requires low black-hole spin. However, for some time, attempts to understand this process were frustrated because it was thought that the Lense–Thirring effect would always quickly co-align a misaligned accretion disk

with the black hole spin (Scheuer & Feiler 1996). In this case, virtually all accretion takes place through a prograde disk, leading to rapid spin-up to high values of the Kerr a parameter. This made it impossible to understand the high SMBH masses referred to above without appealing to initial black hole “seeds” which were themselves already more massive than many SMBH in the low-redshift universe (cf. Volonteri *et al.* 2005). The resolution of this problem was the realization (King *et al.* 2005) that the condition for co- or counter-alignment actually depends on the magnitudes of the disk and black hole angular momenta, and their initial orientation. Scheuer & Feiler’s (1996) paper had implicitly assumed conditions allowing only co-alignment and spin-up. Using the analytic formula of King *et al.* (2005) and assuming sufficiently small feeding events (e.g., limited by self-gravity) shows that most SMBH are likely to have low spins. The exception is a group in giant ellipticals where a direct coalescence of two SMBH has produced a rapid spin (King *et al.* 2008; Fanidakis *et al.* 2009) which subsequent randomized gas accretion is too insignificant to dilute.

It appears that this general picture of small-scale, chaotic accretion events is in reasonable accord with observations of AGN. However reproducing these conditions theoretically is a challenge for models of the feeding process (cf. Hopkins & Quataert 2009). Similarly, the mechanics of the accretion disk itself, particularly its innermost parts, is the subject of intense research. At a fundamental level, it is now almost universally agreed that magnetic fields are implicated in the “viscous” process, removing angular momentum from disk material and causing it to accrete (Balbus & Hawley 1991). However numerical implementations of this idea are not yet definitive (cf. King *et al.* 2007). Simulations using the shearing-box approximation appear to suggest that angular momentum removal becomes less efficient as numerical resolution is increased (Fromang & Papaloizou 2007), and as yet no simulation appears to give viscosity as large as that deduced from observation without making the assumption of a net vertical magnetic field (King *et al.* 2007). Given these theoretical problems in describing disk accretion, we are still some distance from a deterministic picture of it.

3. Outflows

All galaxies are likely to go through active phases as they grow by mergers. Given the rarity of active galaxies among all galaxies, these phases must be relatively short. Accordingly, AGN must feed at fairly high rates to grow the observed high SMBH masses. There is no obvious reason why these rates should respect the black hole’s Eddington limit, so outflows driven by continuum radiation pressure are a natural consequence. This is an encouraging deduction, as outflows driven by black holes offer a simple way of establishing relations between the SMBH and its host galaxy, and hence potential explanations for the M – σ and M – M_{bulge} relations (Ferrarese & Merritt 2000; Gebhardt *et al.* 2000; Häring & Rix 2004).

However it is clear from equation (1.6) that the Eddington ratio \dot{m} is limited to modest values in AGN \dagger . The electron scattering optical depth τ in a quasi-spherical super-Eddington wind scales linearly with \dot{m} , and is of order unity for $\dot{m} \sim 1$. This low scattering depth implies that the total momentum of a $\dot{m} \sim 1$ AGN wind must be of order

\dagger This contrasts strongly with accretion in stellar-mass binary systems because their very short dynamical timescales (approximately an orbital period) allow extremely high dynamical mass transfer rates and hence $\dot{m} \gg 1$ — for example, the well-known binary SS 433 has $\dot{m} \sim 5000$ (cf. King *et al.* 2000; Begelman *et al.* 2006).

the photon momentum (King & Pounds 2003), i.e.,

$$\dot{M}_{\text{out}}v \approx \frac{L_{\text{Edd}}}{c}, \tag{3.1}$$

as is, for example, also found for the winds of hot stars. Using equation (2.3) with $L_{\text{acc}} = L_{\text{Edd}}$ in equation (3.1) gives the wind velocity

$$v \approx \frac{\eta}{\dot{m}}c \sim 0.1c. \tag{3.2}$$

Since the wind moves with speed $\sim 0.1c$, it can persist long after the AGN is observed to have become sub-Eddington. The duration of the lag is $\sim 10R/c$, where R is the radial extent of the wind. For $R > 3$ pc, this lag is at least a century, and far longer lags are possible, as we shall see. This may be the reason why AGN showing other signs of super-Eddington phenomena (e.g., narrow-line Seyfert 1 galaxies) are nevertheless seen to have sub-Eddington luminosities (e.g., NGC 4051: Denney *et al.* 2009).

With equation (3.2), the mass conservation equation for the outflow gives the combination $NR^2 = \dot{M}_{\text{out}}/4\pi v$, specifying the ionization parameter

$$\xi = \frac{L_i}{NR^2} \tag{3.3}$$

of the wind. Here $L_i = l_i L_{\text{Edd}}$ is the ionizing luminosity, with $l_i < 1$ a dimensionless parameter specified by the quasar spectrum, and $N = \rho/\mu m_p$ is the number density. This gives

$$\xi = 3 \times 10^4 \eta_{0.1}^2 l_2 \dot{m}^{-2}, \tag{3.4}$$

where $l_2 = l_i/10^{-2}$, and $\eta_{0.1} = \eta/0.1$.

Equation (3.4) shows that the wind momentum and mass rates determine its ionization parameter: for a given quasar spectrum, the predominant ionization state is such that the threshold photon energy defining L_i , and the corresponding ionization parameter ξ , together satisfy equation (3.4). This requires high excitation: a low threshold photon energy (say, in the infrared) would imply a large value of l_2 , but the high value of ξ then given by equation (3.4) would require the presence of very highly ionized species, physically incompatible with such low excitation. For a typical quasar spectrum, an obvious self-consistent solution of equation (3.4) is $l_2 \approx 1$, $\dot{m} \approx 1$, $\xi \approx 3 \times 10^4$. This corresponds to a photon energy threshold appropriate for helium-like or hydrogen-like iron (i.e., $h\nu_{\text{threshold}} \sim 9$ keV). We conclude that *Eddington winds from AGN are likely to have velocities $\sim 0.1c$, and show the presence of helium-like or hydrogen-like iron.*

A number of such winds are known (for a review, see Cappi 2006). This section shows that it is no coincidence that in all cases the wind velocity is $v \sim 0.1c$, and further that they are all found by identifying blueshifted resonance lines of Fe XXV and Fe XXVI in absorption. Conversely, any observed wind with these properties automatically satisfies the momentum and mass relations, strongly suggesting launching by an AGN accreting at a slightly super-Eddington rate.

4. Interaction with the Host

It is clear that an Eddington wind of the type discussed above can have a significant effect on its host galaxy. The kinetic power of the wind is

$$\dot{M}_{\text{out}} \frac{v^2}{2} = \frac{v}{2c} L_{\text{Edd}} \approx 0.05 L_{\text{Edd}}, \tag{4.1}$$

where we have used equations (3.1) and (3.2). If the wind persists as the black hole doubles its mass (i.e., for a Salpeter time), its total energy is $\sim 5 \times 10^{59} M_8$ ergs, where M_8 is the black hole mass in units of $10^8 M_\odot$. This formally exceeds the binding energy $\sim M_{\text{bulge}} \sigma^2 \sim 3 \times 10^{58}$ ergs of a galaxy bulge with baryonic mass $M_{\text{bulge}} \sim 10^{11} M_\odot$ and velocity dispersion $\sigma \sim 200 \text{ km s}^{-1}$ (as suggested by the M – M_{bulge} and M – σ relations). Evidently the coupling of wind energy to the galaxy must be inefficient, as black holes would destroy or at least severely modify their host bulges in any significant super-Eddington growth phase. As in the corresponding problem for a stellar wind, the interaction with the host must successively involve an inner (reverse) shock, slowing the central wind, a contact discontinuity between the shocked wind and the shocked, swept-up interstellar medium, and an outer (forward) shock driven into this medium and sweeping it outwards, ahead of the shocked wind (see Figure 1).

The inefficient coupling of wind energy to the galactic baryons noted above strongly suggests that the shocked wind cools rapidly after passing through the inner shock. This removes the thermal pressure generated in the shock, and leaves only the preshock ram pressure acting on the interstellar medium.

The required shock cooling is supplied by the inverse Compton effect of the quasar's radiation field (King 2003). This field typically has Compton temperature $T_c \sim 10^7$ K, whereas the formal temperature at the inner adiabatic shock is $m_p v^2/k \sim 10^{11}$ K. The quasar radiation cools the inner shock efficiently, provided that this is within galaxy-scale distances from the center (King 2003). Inverse Compton cooling should produce a component in the quasar spectrum characterized by $kT_c \sim 1$ keV and with a luminosity $\sim \dot{M}_{\text{out}} v^2/2 \approx 0.05 L_{\text{Edd}}$, i.e., about 5% of the quasar's bolometric output. Note that even if the quasar becomes sub-Eddington, leaving a wind persisting for a lag time $10 R_{\text{shock}}/c$, its radiation field is still able to cool the shock efficiently.

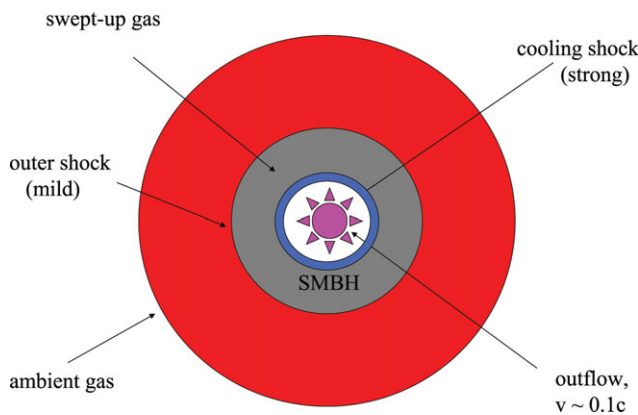


Figure 1. Schematic view of the shock pattern resulting from the impact of an Eddington wind on the interstellar gas of the host galaxy. A supermassive black hole (SMBH) accreting at just above the Eddington rate drives a fast wind (velocity $u = v \sim \eta c \sim 0.1c$), whose ionization state makes it observable in X-ray absorption lines. The outflow collides with the ambient gas in the host galaxy and is slowed in a strong shock. The inverse Compton effect from the quasar's radiation field rapidly cools the shocked gas, removing its thermal energy and strongly compressing and slowing it over a very short radial extent. This gas may be observable in an inverse Compton continuum and lower-excitation emission lines associated with lower velocities. The cooled gas exerts the preshock ram pressure on the galaxy's interstellar gas and sweeps it up into a thick shell (“snowplow”). This shell's motion drives a milder outward shock into the ambient interstellar medium. This shock ultimately stalls unless the SMBH mass has reached the value M_σ satisfying the M – σ relation.

The gas density jumps by a factor ~ 4 at the adiabatic shock, accompanied by a velocity drop by the same factor. It is then strongly compressed in the cooling region while the velocity slows to low values (see Figure 2). Since the cooling is efficient the whole region is very thin compared with the shock radius R_{shock} , and we can regard the shock as locally plane. The Rankine–Hugoniot relations across this isothermal shock then show that the mass flow rate ρv remains constant, while the postshock gas pressure drops to the value

$$P_{\text{ram}} = \rho v^2 = \frac{\dot{M} v}{4\pi b R_{\text{shock}}^2} \approx \frac{L_{\text{Edd}}}{4\pi b R_{\text{shock}}^2 c}, \tag{4.2}$$

i.e., the preshock ram pressure. With a constant cooling time, as expected, the postshock temperature and velocity u drop approximately linearly with distance behind the shock, and the density rises as $1/u$, strongly increasing its emission measure. The gas is likely to be in photoionization equilibrium as it has low optical depth to the quasar radiation, and the increased densities imply short recombination times. The mass conservation equation and ionization parameter (equation 3.3) combine to give

$$\frac{l_i u}{\xi} = \text{constant} \tag{4.3}$$

in this region. *We thus expect a correlation between velocity and excitation.* The rapid cooling in this region implies a rapid transition between the immediate postshock regime ($\sim v/4$, keV excitation) and the much slower and cooler compressed state. There is direct observational evidence for this cooling shock in NGC 4051 (Pounds *et al.*, in preparation). Pounds *et al.* (2004) have already noted a correlation of outflow velocity with ionization in this source.

5. Dynamics

Given the basic structure sketched in the last section, we can investigate how the shock pattern moves through the interstellar medium of the host galaxy. The cooled postshock gas exerts the ram pressure (equation 4.2) on the undisturbed interstellar medium of the galaxy, driving an outer shock into it and sweeping it up into a relatively dense shell of

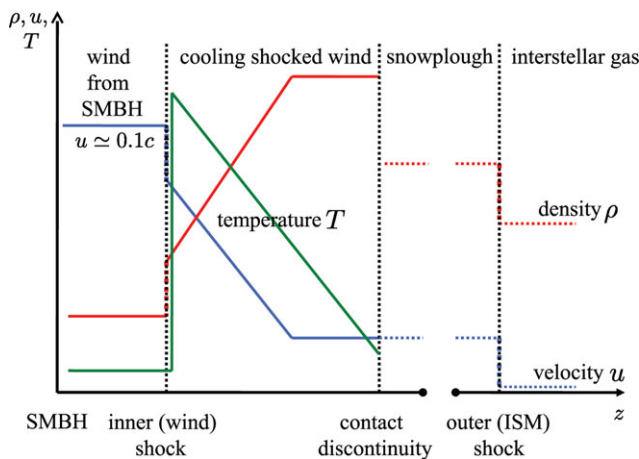


Figure 2. Impact of a wind from an SMBH accreting at a super-Eddington rate on the interstellar gas of the host galaxy: schematic view of the radial dependence of the gas density ρ , velocity u , and temperature T .

increasing mass. The equation of motion of the shell in the momentum-driven limit is

$$\frac{d}{dt}[M(R)\dot{R}] + \frac{GM(R)[M + M_{\text{tot}}(R)]}{R^2} = 4\pi R^2 \rho v^2 = \frac{L_{\text{Edd}}}{c} \quad (5.1)$$

where

$$M(R) = 4\pi \int_0^R \rho_{\text{ISM}} r^2 dr \quad (5.2)$$

is the swept-up interstellar gas mass, M is the black hole mass, $M_{\text{tot}} = M(R)/f_g$ is the total mass within radius R (including any dark matter), and f_g is the gas fraction[†]. Far from the black hole (i.e., for $R > R_{\text{inf}}$) the dark matter term M_{tot} becomes dominant in the equation of motion (5.1), and we can drop the black hole mass term involving M . For a simple isothermal potential, the equation of motion has the analytic solution

$$R_{\text{shock}}^2 = \left[\frac{GL_{\text{Edd}}}{2f_g\sigma^2c} - 2(1 - f_g)\sigma^2 \right] t^2 + 2R_0v_0t + R_0^2 \quad (5.3)$$

where R_0, v_0 are the position and speed of the shell at time $t = 0$ (King 2005). For large times the first term dominates, and the shell can reach arbitrarily large radii if and only if the black hole mass exceeds the critical value

$$M_\sigma = \frac{f_g(1 - f_g)\kappa}{\pi G^2} \sigma^4 \approx \frac{f_g\kappa}{\pi G^2} \sigma^4. \quad (5.4)$$

This is very close to the observed M – σ relation (cf. King 2005). At sufficiently large radii the quasar radiation field is too dilute to cool the wind shock, and the shell accelerates beyond the escape value, cutting off the galaxy and establishing the black-hole mass – bulge-mass relation (cf. King 2003, 2005).

We note that equation (3.1) implies a kinetic energy rate

$$\frac{1}{2}\dot{M}_{\text{out}}v^2 \approx \frac{v}{c}L_{\text{Edd}} \approx \frac{\eta}{2}L_{\text{Edd}} \approx 0.05L_{\text{Edd}}, \quad (5.5)$$

implying a mechanical “energy efficiency” $\eta/2 \approx 0.05$ with respect to L_{Edd} . Cosmological simulations typically adopt such values in order to produce an M – σ relation in agreement with observations (e.g., Di Matteo 2005). This implicitly means that they adopt the single-scattering momentum relation (equation 3.1). We shall see below that there must also be an implicit assumption of momentum rather than energy driving, i.e., that the wind interacts with the host galaxy through its ram pressure rather than its energy.

6. Energy-Driven Outflows

We see from the reasoning of the last section that the interaction between the quasar wind and its host establishing the M – σ relation is — crucially — “momentum-driven” rather than “energy-driven”. This equivalent to requiring efficient shock cooling. An energy-driven shock (e.g., Silk & Rees 1998) would result in a much smaller black hole mass for a given σ than observed. Instead of the momentum rate L_{Edd}/c balancing the weight of swept-up gas $4f_g\sigma^4/G$, which is what produces the momentum-driven relation (equation 5.4), an energy-driven shock would equate the energy deposition rate to the rate of working against this weight. In the near-Eddington regime, the result is

$$\frac{1}{2}\dot{M}_{\text{out}}v^2 \approx \frac{\eta}{2}L_{\text{Edd}} = 2\frac{f_g\sigma^4}{G} \cdot \sigma, \quad (6.1)$$

[†] Note that in equation (2) of King (2005), the suffix “tot” was inadvertently missed off the relevant quantity.

i.e.,

$$M(\text{energy}) \approx \frac{2f_g \kappa}{\eta \pi G^2 c} \sigma^5 = \frac{2\sigma}{\eta c} M_\sigma = 3 \times 10^6 \sigma_{200}^5 M_\odot, \tag{6.2}$$

which lies well below the observed relation. The coupling adopted in cosmological simulations evidently ensures that the interstellar medium feels the outflow momentum rather than its energy, in addition to the “energy efficiency” $\sim \eta/2 \approx 0.05$ noted above.

7. Galaxy-Wide High-Velocity Outflows

On large scales, the outflows described in §5.2 above all have (outer) shock velocities limited by the bulge velocity dispersion σ . Yet optical and UV observations of various types of galaxies (Holt *et al.* 2008; Tremonti *et al.* 2007) give clear evidence of outflows with velocities of several times this value. These cannot be the central quasar winds with $v \sim 0.1c$ discussed in §3.

There is a simple interpretation of such large-scale high-velocity outflows. Consider a galaxy in which the SMBH has reached the mass M_σ given by equation (5.4), with the cosmic gas fraction $f_g \approx 0.16$. Its bulge gas will probably be severely depleted. In a subsequent minor accretion event triggering AGN activity, the effective gas fraction in the bulge will be $f'_g < f_g$. If accretion on to the SMBH becomes super-Eddington for a time $> 10^5$ yr, the AGN must drive an outflow shock beyond the radius R_{inf} . However, because of the discrepancy between f_g (establishing the black hole mass) and f'_g (the current gas fraction), the shell radius now obeys a modified form of the analytic solution (5.3), namely

$$R_{\text{shock}}^2 = \left[\frac{GL_{\text{Edd}}}{2f'_g \sigma^2 c} - 2(1 - f'_g)\sigma^2 \right] t^2 + 2R_0 v_0 t + R_0^2, \tag{7.1}$$

where the L_{Edd} term involves f_g rather than f'_g . Thus at large t we have

$$R_{\text{shock}}^2 = 2 \left[\frac{f_g}{f'_g} (1 - f_g) - (1 - f'_g) \right] \sigma^2 t^2 \approx 2 \frac{f_g}{f'_g} \sigma^2 t^2, \tag{7.2}$$

where we have taken $f'_g \ll f_g < 1$ in the last form. This shows that the shell reaches velocities

$$\approx (2f_g/f'_g)^{1/2} \sigma > \sigma, \tag{7.3}$$

because its inertia is much lower than the one previously expelled by the Eddington thrust in the accretion episode which defined the SMBH mass. If at some point the AGN activity turns off, we can match another solution of the form of equation (5.3), but with L_{Edd} formally equal to zero, to the solution given by equation (7.1). This solution reveals that a coasting shell stalls only at distances $\sim (f_g/f'_g)^{1/2}$ times its radius R_0 at the point when AGN activity ceased, and thus persists for a timescale $R_0/\sigma \sim 10^8$ yr.

Episodic minor accretion events of this type therefore naturally produce large-scale outflows with velocities $> \sigma$. Moreover, since they persist as fossil winds long after the AGN has become faint, they can have total momentum considerably higher than could be driven by the *current* AGN radiation pressure, i.e., well in excess of the apparent momentum limit. A recent paper (King 2009) gives more details of the expected outflows.

8. Conclusion

AGN accretion appears to involve a series of very small-scale, chaotic events, whose gas flows have no correlation with the large-scale structure of the galaxy or with each other.

The accreting gas has extremely low specific angular momentum and is presumably only a small fraction of the gas involved in a galaxy merger.

The growth of SMBH through accretion requires Eddington accretion episodes in AGN to be common. Mass and momentum conservation then imply winds with velocities $v \sim 0.1c$ and the presence of resonance lines of helium-like and hydrogen-like iron. The wind shocks and cools as it interacts with the interstellar medium of the host galaxy, and may be observable in an inverse Compton continuum and lower-excitation emission lines with lower velocities. The shocked wind begins to sweep up the galaxy ISM once the black hole mass reaches the value M_σ implied by the M - σ relation, preventing growth beyond this mass. If the shocked gas did not cool as stated above, the resulting (“energy-driven”) outflow would imply a far smaller SMBH mass than actually observed. Minor accretion events with small gas fractions can produce galaxy-wide outflows, including fossil outflows in galaxies where there is little current AGN activity.

Acknowledgements

I thank Ken Pounds and Sergei Nayakshin for illuminating discussions and the Royal Society for a travel grant.

References

- Balbus, S. A. & Hawley, J. F. 1991, *ApJ*, 376, 214
 Barth, A. J., Martini, P., Nelson, C. H., & Ho, L. C. 2003, *ApJ*, 594, L95
 Begelman, M. C., King, A. R., & Pringle, J. E. 2006, *MNRAS*, 370, 399
 Cappi, M. 2006, *AN*, 327, 1012
 Denney, K. D., *et al.* 2009, *ApJ*, 702, 1353
 Di Matteo, T., Springel, V., & Hernquist, L. 2005, *Nature*, 433, 604
 Fanidakis, N., Baugh, C. M., Benson, A. J., Bower, R. G., Cole, S., Done, C., & Frenk, C. S. 2009 [arXiv:0911.1128]
 Ferrarese, L. & Merritt, D. 2000, *ApJ*, 539, L9
 Fromang, S. & Papaloizou, J. 2007, *A&A*, 476, 1113
 Gebhardt, K., *et al.* 2000, *ApJ*, 539, L13
 Häring, N. & Rix, H.-W. 2004, *ApJ*, 604, L89
 Holt, J., Tadhunter, C. N., & Morganti, R. 2008, *MNRAS*, 387, 639
 Hopkins, P. F. & Quataert, E. 2009 [arXiv:0912.3257]
 King, A. 2003, *ApJ*, 596, L27
 King, A. 2005, *ApJ*, 635, L121
 King, A. R. 2009, *MNRAS*, in press [arXiv:0911.1639v1]
 King, A. R., Lubow, S. H., Ogilvie, G. I., & Pringle, J. E. 2005, *MNRAS*, 363, 49
 King, A. R. & Pounds, K. A. 2003, *MNRAS*, 345, 657
 King, A. R. & Pringle, J. E. 2006, *MNRAS*, 373, L90
 King, A. R. & Pringle, J. E. 2007, *MNRAS*, 377, L25
 King, A. R., Pringle, J. E., & Hofmann, J. A. 2008, *MNRAS*, 385,
 King, A. R., Taam, R. E., & Begelman, M.C. 2000, *ApJ*, 530, L25
 Kinney, A. L., Schmitt, H. R., Clarke, C. J., Pringle, J. E., Ulvestad, J. S., & Antonucci, R. R. J. 2000, *ApJ*, 537, 152
 Pounds, K. A., Reeves, J. N., King, A. R., & Page, K. L. 2004, *MNRAS*, 350, 10
 Scheuer, P. A. G. & Feiler, R. 1996, *MNRAS*, 282, 291
 Shakura, N. I. & Sunyaev, R. A. 1973, *A&A*, 24, 337
 Silk, J. & Rees, M. J. 1998, *A&A*, 331, L1
 Tremonti, C. A., Moustakas, J., & Diamond-Stanic, A. M. 2007, *ApJ*, 663, L77
 Volonteri, M., Madau, P., Quataert, E., & Rees, M. J. 2005, *ApJ*, 620, 69
 Willott, C. J., McLure, R. J., & Jarvis, M. J. 2003, *ApJ*, 587, L15